

## DIRECTIVITY ANALYSIS OF SOUND IN TURBULENT EXHAUST JETS WITH LAMINAR CROSS-FLOW: A NUMERICAL STUDY

Orddom Y Leav<sup>1</sup>, Benjamin S Cazzolato<sup>1</sup> and Carl Q Howard<sup>1</sup>

<sup>1</sup>School of Mechanical Engineering  
University of Adelaide Australia, Adelaide SA 5005, Australia  
Email: [orddom.leav@adelaide.edu.au](mailto:orddom.leav@adelaide.edu.au)

### Abstract

It is commonly assumed directivity of sound from exhaust stacks is axisymmetric, which is a reasonable assumption below cut-on and in the absence of flow or elevated stack temperatures. This paper shows that the sound directivity is non-spherical when there is a laminar cross-flow across the outlet of an exhaust stack that ejects hot subsonic gas. This computational study uses computational fluid dynamics to model the heated jet exhausting into a mean laminar cross-flow and the linearised Euler equations, solved using the finite element method, to model the propagation of sound. This non-spherical spreading is due to the refraction of sound in the shear layer and diffraction at the edge of the stack outlet. Furthermore, the laminar mean cross-flow causes asymmetric spreading of the acoustic field, as the exhaust flow is also non-axisymmetric. The implications of these findings suggest that community noise level predictions from stacks may be under-predicted due to the altered directivity of the exhaust stack caused by cross-flow and refraction effects from hot exhaust gases.

### 1. Introduction

Open cycle gas turbines (OCGT) are increasingly used for power generation as they are able to provide base loads in peaking or uncertain conditions and can respond quickly to power grid demands. However, some have been found to produce significantly higher community noise levels than is predicted using ISO Standard 10494 [1]. This issue of excessively high levels of low frequency noise from OCGT has been well documented internationally [2], [3], [4]. These excess levels of low frequency noise from OCGT can have the following effects: perceived annoyance of ‘throbbing’ from high intensity low frequency noise [3], ‘beating’ sensation in the chest [5], nausea [3] and acoustic excitation in structures with low resonant frequency, such as glass structures and wall panels [3]. The causes for the increased levels of low frequency noise in communities near OCGT is the subject of ongoing research. The source of excess low frequency noise from OCGT should be investigated in further detail in order to assist in the planning stages of such systems, as well as for the design of noise mitigation.

Currently, the ISO Standard 10494 for gas turbines assumes that the sound directivity from an exhaust stack is primarily from diffraction and does not take into consideration the flow effects [5]. In heated turbulent exhaust jets, flow mechanisms such as pressure gradient and temperature gradients in the shear layer can alter the sound propagation. Early research into the interaction of sound with a jet’s shear layer has shown that plane waves will refract in an infinitesimally thin shear layer [6]. This work was expanded by the experimental work of Candel [7], and theoretical models developed by Cargil [8], which have shown that sound refraction occurs in a finite thickness shear layer. Further studies conducted by various other researchers into the phenomenon of shear layer refraction in jets has shown

that with modest Mach numbers ( $M=0.1$ ) large dips (in excess of 20dB) in the directivity of the jet's centre line were observed [9], [10], [11]. Other effects such as radiation, scattering, reflections and acoustic spectrum broadening are also present in the shear layer's pressure gradient. The temperature gradients in the jet can also supplement the pressure gradient effects in the shear layer [12].

The presence of laminar cross-flow with turbulent exhaust jets is commonly seen in turbulent exhaust stacks and is a well-researched topic. The jet in cross-flow (JICF) problem is also seen in various applications such as oil film cooling for turbine blades, fuel injectors and dilution holes in gas turbine combustors [13]. Experimental analysis and computational fluid dynamics (CFD) simulations has shown that three-dimensional JICF can generate flow features such as shear layers, counter rotating vortex pairs, wake vortices and horse shoe vortices [13]. These features are not present in two-dimensional JICF where a recirculation zone forms on the leeward side of the exhaust jet instead [14], [15]. An additional feature that is present in two-dimensional JICF studies and not in three-dimensional JICF is the reattachment of the wake downstream [14], [15]. From the literature previously stated it is evident that shear layer and pressure gradient will cause refraction.

This paper analyses the effects that the thermal mixing of a hot turbulent jet exhaust with a cold laminar cross-flow has on the sound directivity of a turbulent subsonic heated exhaust stack. This study will use two-dimensional CFD and finite element analysis (FEA) to investigate the sound directivity in the following two scenarios: infinitely baffled infinitely thin rectangular (ribbon) pistons and heated JICF. The layout of the paper is as follows. The simplified computational model and boundary conditions of the computational mesh will be discussed in Section 2. Subsequently, the mathematical models that are used for the fluid flow simulations through CFD and acoustic propagation using linearised Euler equations (LEE) with FEA are explained. The analytical and simulation results from CFD and FEA are presented in Section 4, which shows the numerical fluid dynamics solution and the effects of temperature on the propagation of sound. The main conclusions of this paper and proposed future work are summarised in Section 5.

## **2. Details of Computational Model**

### **2.1 Simplifications of the Computational Model**

In this paper the complexity of modelling a realised OCGT exhaust stack has been simplified to ensure the modelling is computationally feasible. A schematic for simplified model is shown in Figure 1. Firstly, the computational model has been reduced to a two-dimensional simulation with an infinitely thin rectangular duct with finite length. The duct in the simulation is modelled as a straight duct with rigid no-slip walls. In a real exhaust stack the outlet of duct has finite dimension and contains complex geometries in the system such as baffles for sound attenuation, contractions, bends and other flow noise inducing mechanisms. Adjacent to the duct outlet is a half-space with a rigid reflective ground, which are similar to various studies previously completed [14],[15]. This assumption is adequate in analysing the basic fluid structures and reducing the complexity of the problem, but in reality the ducts are protruding and the flow in leeward side of the jet are not bounded by an adjacent wall. Since, the simulation is two-dimensional three-dimensional effects such as eddy formation, three dimensional flow features as described in Section 2.4.1 and three dimensional hemispherical spreading of sound cannot be captured in the simulation. A key limitation of this model is that sound is only generated from the harmonic source at the inlet and other flow generating mechanisms are neglected. Nevertheless, these limitations have been taken into consideration and the overall trend in sound propagation through thermal distribution of a jet in cross-flow can be ascertained.

In order to directly quantify the effects of the JICF it is essential to model the sound propagation with and without effects of flow and temperature. This study investigates the propagation of sound from a baffled infinitely thin rectangular piston with the absence of flow as the benchmark case. This benchmark case has well known trends for planar sources with low Helmholtz numbers and frequencies well below cut-on frequency. Subsequent sound propagation modelling initially involved CFD modelling for convective bulk fluid flow to generate the temperature distribution. The calculated temperature field is applied to the FEA model, which is used to vary the speed of sound appropriately.



### 2.2.1 Outlet and Far-Field Boundary Conditions

In the far-field of the CFD model there are two different outlet conditions that are used. The first outlet condition is a free-slip wall boundary condition in the normal direction to the wall attached to the duct outlet and perpendicular to the cross-flow inlet. This was chosen to allow the shear stress along the wall to be zero. This is the same as implementing a symmetry boundary condition. At the domain outlet, parallel to the cross-flow velocity inlet a pressure outlet condition is used. The temperature at the pressure outlet boundary condition was set to the same temperature as the cooler cross-flow inlet of 300K.

For the computational sound propagation simulation, the far-field condition is uniform for all boundary conditions. Perfectly matching layer (PML) elements are used for the far-field absorption of sound to simulate the half-space. The number of PML elements used is dependent on the duct width,  $D$ , and the wavelength of the lower frequency for analysis. Howard and Cazzolato [16] have recommended that the PML zone is at least one-quarter of the wavelength of the lowest frequency interest.

### 2.3 Domain and Meshing Details

The computational domain size for both the CFD and computational acoustic simulation are identical, but the mesh for each simulation differs. The computational domain has been scaled by jet width,  $D$ . The computational domain along the x-axis spans  $256D$  downstream of jet's central axis and  $60D$  upstream from the jet's central axis. The height of the simulation perpendicular to the wall attached to the outlet is  $160D$ . The height and length of the simulation were sufficient to ensure that the majority of critical flow features were captured without effects of the top boundary condition. The large domain size also allows for acoustic measurements in the far-field and to analyse possible mechanisms that may alter the sound propagation path.

For the CFD simulations the mesh (shown in Figure 2) was refined in areas where necessary flow features were to be resolved with structured hexahedrals elements. This mesh has 726,018 elements and 1,116,520 nodes. The cells with the smallest face area are situated in the duct, near-field region of the duct outlet and in the inflation layer near the bottom wall adjacent to the jet outlet. The non-dimensional wall distance,  $y^+$ , for this simulation is less than 13, which is acceptable for resolving the boundary layer in FLUENT with the scalable wall function. In the duct, geometric near field of the duct outlet and inflation layer elements are generated with structured hexahedras. Structured mesh in this region has a relatively slow growth rate to ensure most of the elements in this region are isotropic to utilise the full capabilities of the third-order discretisation scheme, QUICK. In the geometric far-field where the flow characteristics are of less importance the mesh has been generated with unstructured triangular prism elements. Both element types used in FLUENT only specify nodes at the vertex of the element and is also known as 'brick' elements.

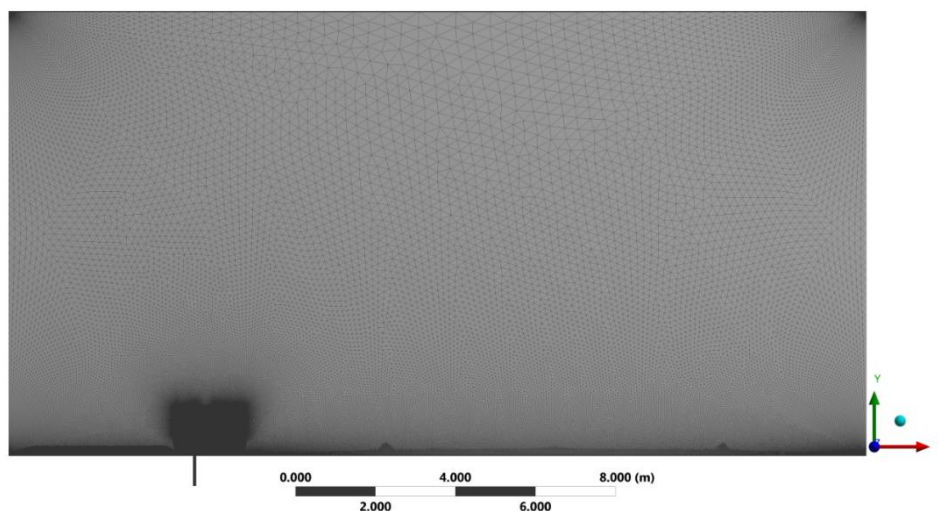


Figure 2. Meshing domain for CFD modelling a baffled rectangular jet with cross-flow

Mesh generation for modelling sound propagation with FEA has different requirements compared to meshing schemes for CFD simulation. Hence, an alternative mesh is necessary for computationally evaluating sound propagation with FEA and the final mesh is shown in Figure 3. In propagating acoustic waves it is desirable to use a structured mesh, ideally aligned in the planar direction of the wave [16]. As a result, the elements from the duct inlet to arcs seen in Figure 3 are structured hexahedra, as is the buffer region and the PML region on the outskirts of computational domain. There is however a small region at the duct outlet which is unstructured hexahedra, but due to the high mesh density and smooth growth rate in element size in that region the effects of the unstructured mesh are minimal. Quadratic FLUID 220 acoustic elements are used in the simulation. According to Howard and Cazzolato [16], at least six elements per wavelength are required for accurately resolving the acoustic pressure wave. Therefore, for the mesh shown in Figure 2 the maximum Helmholtz number achievable for this simulation is 0.66, and consequently all calculations will be conducted at Helmholtz numbers less than 0.6. The resulting acoustic element count is 448,484 and node count is 3,151,801.

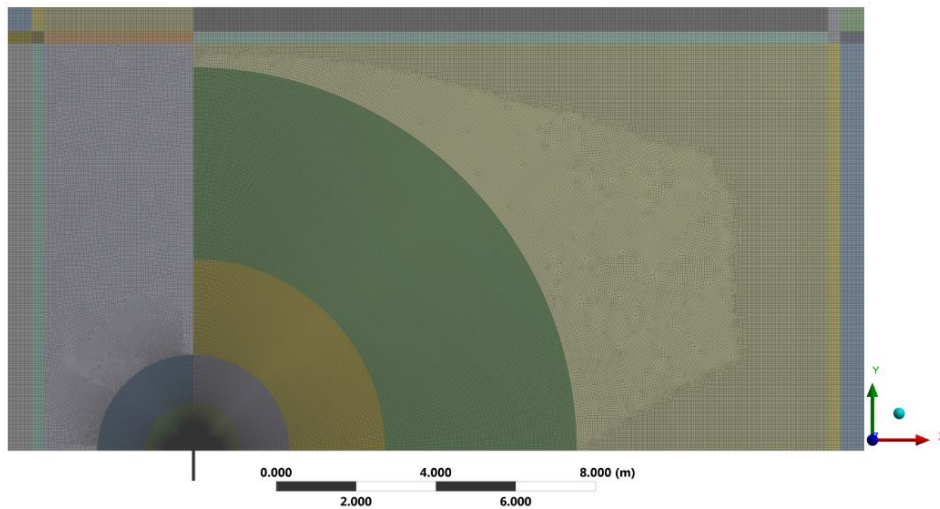


Figure 3. Meshing domain for acoustic FEA modelling sound propagation in a baffled duct with

## 2.4 Mathematical Models

This section will discuss the equations and models for both the CFD and sound propagation simulations.

### 2.4.1 Governing Models for Computational Fluid Mechanics

The fluid dynamics of the two-dimensional jet in cross-flow was simulated using ANSYS FLUENT [17]. The fluid flow in the model was computationally resolved using the compressible steady Reynolds Averaged Navier Stokes Equation (RANS). The fluid medium for this analysis is dry air. The density for the simulation was resolved using the ideal gas assumption for compressible analysis. The viscosity of the model was also calculated using the Sutherland approximation. The simulation also assumes the jet is non-buoyant. A pressure based solver with a “Coupled” setting for the pressure-velocity coupling was chosen. The spatial, pressure, energy and turbulent discretisation schemes chosen were a combination of the third-order QUICK scheme in isotropic cells and second-order upwind scheme in non-isotropic cells. The two equation realisable  $\kappa - \epsilon$  model was chosen to resolve the turbulence [18]. This model is computationally less expensive than other more complicated RANS models and scale resolving turbulence models. Furthermore, the model is suitable for two-dimensional simulation as it does not resolve the three-dimensional eddies directly. However, there are limitations in the turbulence model: it assumes the eddy viscosity is isotropic; the turbulence can be modelled with two equations; the eddies in the models are not resolved with the average turbulence quantities being calculated in the shear layer; lack of prediction for flow separation at the jet inlet edge; and inaccurate prediction of the jet spreading and decay [18]. The boundary layer in the no-slip walls in the

model were resolved using scalable wall functions. For the CFD analysis in this paper, only the critical features of the flow will need to be reproduced and the compressible steady RANS model is sufficient.

### 2.4.2 Sound Propagation using Finite Element Analysis

Sound propagation simulations were conducted with ANSYS Mechanical by solving the LEE with FEA [19]. This type of analysis requires an Acoustic ACT extension to be used for solving these types of simulations [19]. In solving the LEE the following assumptions are made: the air medium is compressible, there are no mean flow on the fluid, the changes in density are small in comparison to the mean density, the viscous dissipation of the fluid is neglected and the acoustic pressure can be represented by the wave equation. Harmonic analyses were chosen for this modelling work, as it allows the system to be driven by a sinusoidal oscillating harmonic source. The elements in this simulation are set with the symmetric algorithms for faster solution times and is possible with the absence of fluid structural interaction between the propagated sound and the boundary conditions. The elements at the duct are set with the coupled symmetric algorithm to allow the fluid structure interaction at the inlet for acoustic source definition. The elements in the remaining domain are set with uncoupled symmetric algorithm. As discussed in Section 2.3, the higher order FLUID 220 elements are used for the simulation. Since, the model has large temperature gradients, the convective effects are neglected, as they only correspond to 10% of the temperature effects and will have little impact on the results.

## 3. Computational Results

### 3.1 Baffled Infinitely Thin Rectangular Piston

The acoustic radiation of a baffled infinitely thin rectangular piston was simulated and the results were used as a benchmark scenario for sound propagation in absence of heated flow. The results indicate that in the absence of heated flow the acoustic spreading from the duct outlet is spherical at the Helmholtz numbers of interest, as shown in Figure 4. This is to be expected of Helmholtz numbers significantly less than one and the frequency of the harmonic planar source is less than cut-on frequency of the duct. The computational acoustic power results in the far-field have also been compared with the acoustic power results from the methods used in the standard ISO 10494 [5]. Computational acoustic power results at a Helmholtz number of 0.3, in the far-field is approximately 103.0dB ref  $10^{-12}$  W, whereas the acoustic power from the standards is 103.1dB ref  $10^{-12}$  W. Since, the difference is minimal it can be concluded that the standards are adequate in estimating the sound power for sound propagation in exhaust stacks without heated flow. This has also been confirmed for higher Helmholtz numbers of up to 0.6.

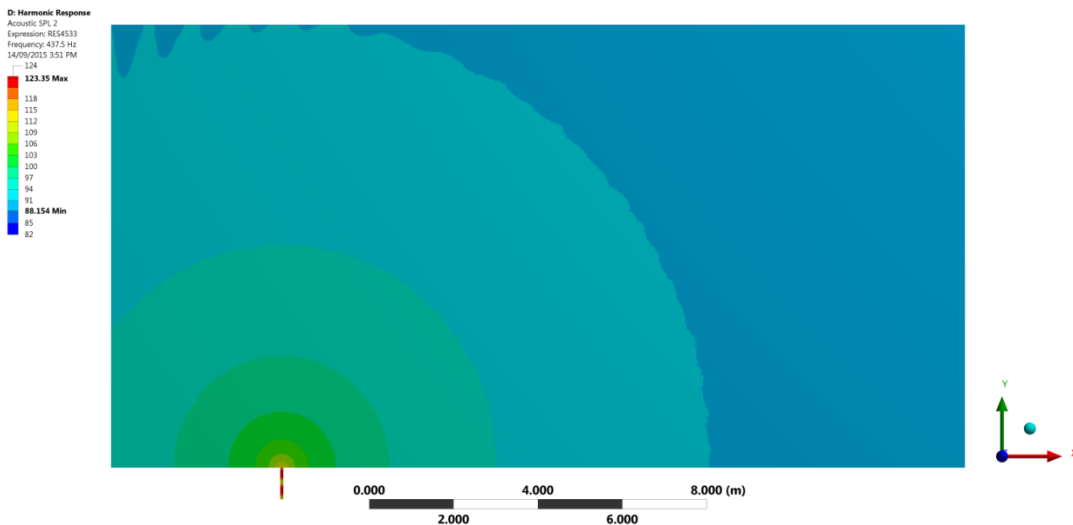


Figure 4. Acoustic SPL contour plot for a Helmholtz number of  $ka = 0.3$  in the absence of flow

### 3.2 Heated Rectangular Jets in Cross-flow

#### 3.2.1 Fluid Flow Features of Heated Rectangular Jets in Cross-Flow

The CFD simulation results for an infinitely thin heated rectangular JICF conducted in this study displays distinct flow features that have been witnessed in previous incompressible and ambient temperature studies. The velocity magnitude results from the CFD simulation are portrayed in Figures 4 and 5 with velocity streamlines and velocity vectors, respectively. These velocity streamlines in Figure 5 originate from either the turbulent jet inlet or laminar cross-flow inlet. A distinct feature seen in Figure 5 is that there is a strong curvature in the jet, as a result of the cross-flow and a reattachment region further downstream. Since the velocity streamlines only display the streamlines originating from the inlets, there is a region near the jet outlet that is missing in Figure 5, but can be seen in the velocity vector results, shown in Figure 6. The distinct recirculation in this region is a contributing factor in the curvature and reattachment of the jet with the adjacent wall. These features are also observed in the incompressible and ambient temperature experimental study by Mikhail, Chu and Savage [15], and numerical study by Kavsaoglu and Akmandor [14]. Therefore, the CFD simulations conducted in this research have produced similar results to previous studies, and the presence of compressibility and temperatures have minor effects on the dominant flow features.

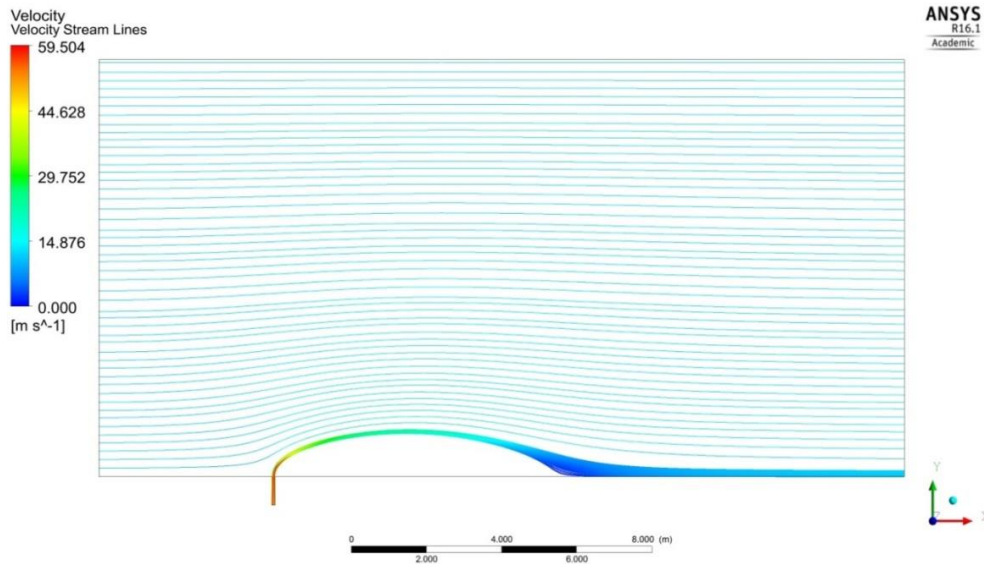


Figure 5. Two-dimensional JICF velocity streamline plot

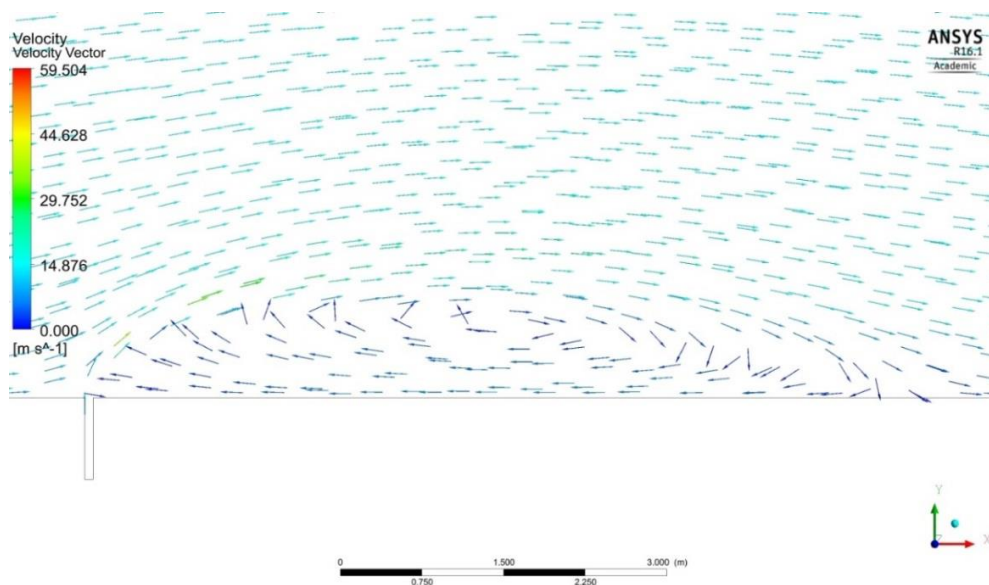


Figure 6. The velocity vector plot for the two-dimensional JICF in the recirculation region

The thermal results for the absolute temperature of the simulation show a dependence on the distinct convective flow features. The temperature distribution of the simulation is depicted with a temperature contour plot shown in Figure 7, where it is clearly shown that the region near the jet outlet possess the highest temperature. As the heated jet propagates further downstream entrainment with the cooler cross-flow occurs and the temperature of the overall plume continually decreases. There is also a strong correlation with the deflection of high temperature fluid in Figure 7 and the curvature in the velocity streamlines seen in Figure 5. It is also seen in Figures 6 and 7 that in the recirculation zone there are local minimums in both the velocity magnitude and temperature. Furthermore, the temperature gradients on the leading and leeward side of the plume are also correlated with the velocity gradient in the shear layer. Hence, there is evidence to suggest that the temperature distribution of the infinitely thin heated jet in cross-flow is dependent on the convective fluid flow.

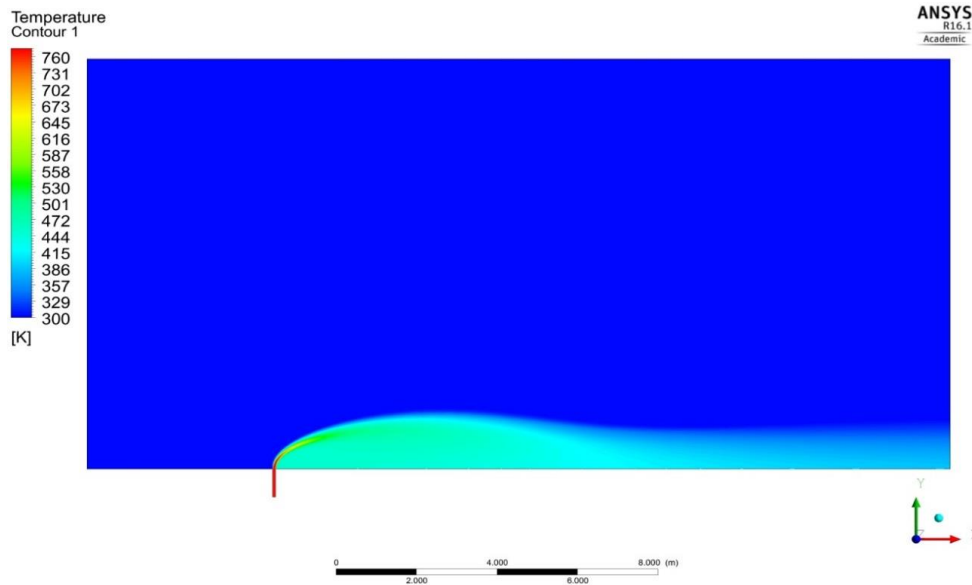


Figure 7. The temperature contour plot for the heated JICF

### 3.2.2 Sound Directivity of Heated Rectangular Jets in Cross-Flow

The thermal distribution from the CFD simulation was imported into the FE model and applied to the nodes. The FEA software models sound generation and propagation through the LEE, as described in Section 2.3.2. The resulting SPL for a Helmholtz number of 0.3 are shown in Figure 8. The SPL contour plot can be compared to Figure 4 where a significant change in the propagation path of sound can be seen. In the absence of temperature variation, the propagation of sound at these Helmholtz numbers exhibit hemi-spherical spreading from the duct outlet, as discussed in Section 3.1. However, this is not the case with the temperature distribution present and there are two distinct lobes forming. The lobe on the windward side of the jet is predominantly elliptical. On the leeward side the lobe is highly directive and is related to the deflected jet. With the presence of the temperature effects there is a strong increase in the sound levels perpendicular to the centre jet axis. Further downstream, sound is being reflected off the bottom wall and is ‘beaming’ off the wall. This reflection of sound is strongly dependant on the reattachment of the plume. The formation of the distinct lobes in relative near-field is from the refraction of sound in the temperature gradient, however in the far-field is a combination of directly refracted field and reflect field from the ground. The sound power has also been calculated based on the standards and compared with the numerical sound power in the far-field at a Helmholtz number of 0.3. The sound power based on the far-field numerical measurements and standards are 103.0dB ref  $10^{-12}$  W and 102.8dB ref  $10^{-12}$  W, respectively. Similar to the results in Section 3.1 the standards are sufficiently accurate in estimating the far-field sound power.

In addition to the SPL contour plots, directivity was analysed using normalised SPL polar plots at varying distances from the jet outlet. The result of the polar plot is for a Helmholtz number of 0.3 and is shown in Figure 9. The SPLs were normalised by the on-axis SPL for the simulation in the absence of the jet. The SPL results are taken from six different radial distances from the jet and have

been scaled with  $D$ . It can be seen in Figure 9 the normalised SPL in the absence of flow is relatively spherical for varying distances from the jet outlet, but this is definitely not the case with the thermal effects present. The results in the polar plot show that with increasing radial distances from the jet there are increases in the normalised SPL of the two side lobes. In particular, the normalised SPL in the side lobe of the leeward side of the JICF seems to be directly related to the radial distance with the results at  $128D$  showing the largest lobe. There are also evidence of the reflective effects from the bottom wall in far-field ( $128D$ ) and not in the relative near-field. From the analysis it can be seen that the normalised SPL for two-dimensional JICF are highly dependent on the radial arc of measurement. However, the normalised SPL for exhaust stacks without heated flow have relatively spherical distribution at most of the radial arcs in this study. As a result of the normalised SPL polar plots it can be seen that the thermal effects from the two-dimensional JICF has significantly altered sound propagation path and the results are strongly dependent on the radial location for measurements which is consistent with previous studies on sound propagation of sound in unheated axis-symmetric jets [9].

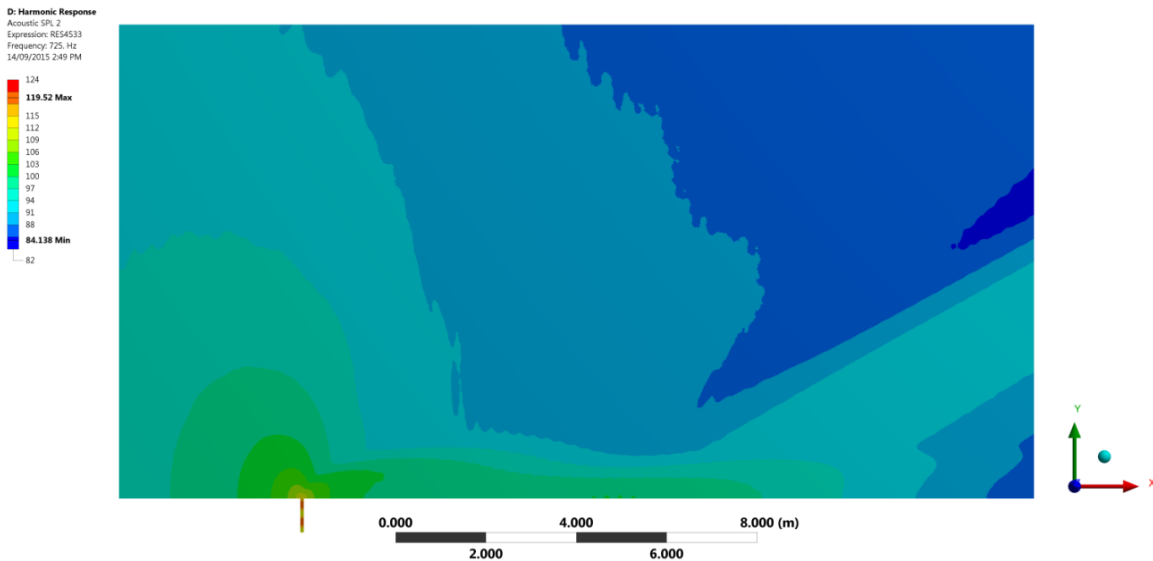


Figure 8. Acoustic SPL contour plot for a  $ka = 0.3$  with the thermal distribution from the JICF

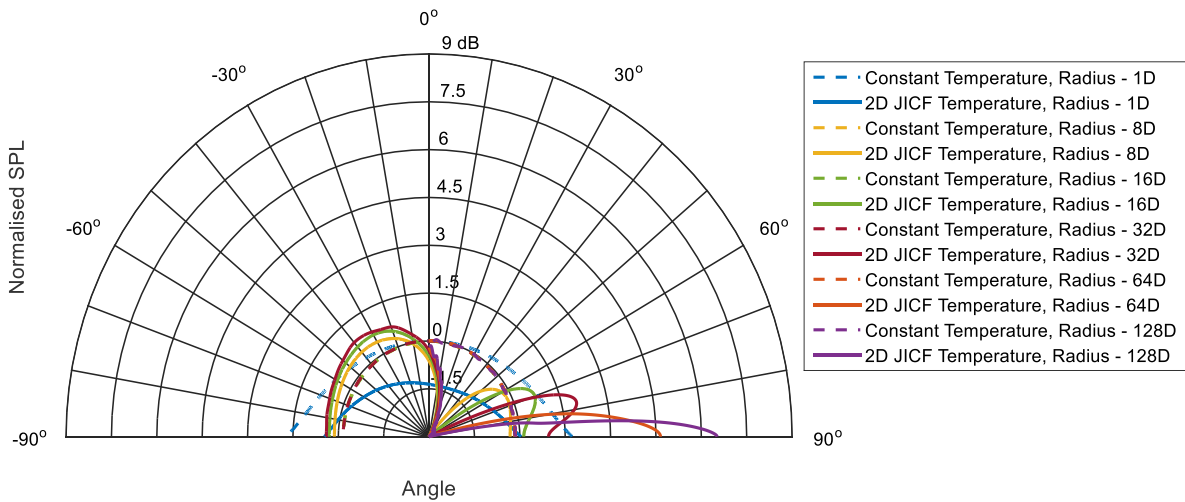


Figure 9. Normalised SPL polar plot at a  $ka = 0.3$  with and without the thermal effects from the JICF

#### 4. Conclusions and Future Work

The results from this study's simulations has shown that the temperature gradients from two-dimensional JICF can greatly affect the directivity of sound. The results have clearly indicated that in the absence of heated flow the propagation of sound from the duct is spherical. However, this is not the case with the temperature gradient from the two dimensional JICF, where the sound propagation is

now asymmetric due to refraction of the sound waves by the thermal gradients in the shear layer and subsequent edge diffraction at the jet exhaust. Further analysis has shown the normalised SPL is strongly dependant on the radial location of the measurements. Even though the standards are sufficient in calculating the total acoustic power of the system in the far-field, the altered directivity of the two-dimensional JICF has shown that off-axis sound may be under predicted in far field from the cross-flow and refraction effects from hot exhaust gases. The implications of these findings suggest that community noise level predictions from stacks may be under-predicted due to the altered directivity of the exhaust stack.

Future work will be further conducted in this area to build a higher fidelity computational model for better assessing community noise level predictions from OCGT exhaust stacks. The future computational study will involve the following: three dimensional simulations with a finite cylindrical jet, scale resolving simulations to analyse the effects of the vortical structures and resolution of the sound waves using direct computational acoustics. These models will later be validated with experimental test rig, which has been scaled using non-dimensional acoustic parameters.

## References

- [1] ISO 10494:1993 Gas turbines and turbine sets- Measurement of emitted airborne noise – Engineering/survey method, *International Organization for Standardization*, Geneva, Switzerland, 2010.
- [2] Broner, N. “A simple outdoor criterion for assessment of low frequency noise emission”, *Acoustics Australia*, 39, 7-14, (2011).
- [3] Broner, N. “ Power to the people”, *15<sup>th</sup> Int. meeting on low freq. noise & vib. & its control*, *15<sup>th</sup> Int. meeting on low freq. noise & vib. & its control*, Stratford upon Avon, UK, May 2012.
- [4] Hessler Jr, G. F. "Proposed criteria for low frequency industrial noise in residential communities", *Low Frequency Noise, Vibration and Active Control*, **24**, 97-106, (2005).
- [5] Broner, N. “The effects of low frequency noise on people – A review”, *Journal Sound and Vibration*, **58**, 483-500, (1978).
- [6] Amiet, R. K. “Refraction of sound by a shear layer”, *Journal of Sound and Vibration*, **58**, 467-482, (1978).
- [7] Candel, S.M., Julienne, A. and Guedel, A. “ Refraction and scattering of sound in an open wind tunnel flow”, *6<sup>th</sup> International Congress on Instrumentation in Aerospace Simulation Facilities*, 288-300, 1975.
- [8] Cargil, A.M. “Low frequency acoustic radiation from a jet pipe – a second order theory”, *Journal of Sound and Vibration*, **83**, 339-354, (1982).
- [9] Mungur, P., Plumblee, H.E., and Doak, P.E., “Analysis of acoustic radiation in a jet flow enviroment”, *Journal Sound and Vibration*, **68**, 21-52, (1974).
- [10] Savkar, S.D., “Radiation of cylindrical duct acoustic modes with flow mismatch”, *Journal Sound and Vibration*, **42**, 363-386, (1975).
- [11] Maestrello, L., Bayliss, A. and Turkel, E., “On the interaction of a sound pulse with the shear layer of an axisymmetric jet”, *Journal Sound and Vibration*, **74**, 281-301, (1981).
- [12] Candel, S.M., “Acoustic transmission and reflection by a shear layer discontinuity separating hot and cold regions”, *International Journal of Aeroacoustics*, **8**, 199-230, (1972).
- [13] Kelso, R.M., Lim, T.T. and Perry A.E., “An experimental study of round jets in crossflow”, *Journal of Fluid Mechanics*, **306**, 111-144, (1996).
- [14] Kavsaoglu, M.S. and Akmandor I.S., “Navier-Stokes simulation of two and three dimensional jets in crossflow”, *American Institute of Aeronautics and Astronautics*, 1-20, (1991).
- [15] Mikhai vgl, R., Chu, V.H. and Savage, S.B., “ The reattachment of a two-dimensional turbulent jet in confined crossflow”, *Proceedings of the 16<sup>th</sup> IAHR Congress*, Sao Paulo, Brazil, **3**, 414-415, (1975).
- [16] Howard, C.Q. and Cazzolato, B.S. *Acoustic analysis using MATLAB and ANSYS*, CRC Press, 2014.
- [17] ANSYS, *ANSYS FLUENT*, ver. 16.1, computer program, ANSYS Inc, Canonsburg, Pennsylvania, 2015.
- [18] Shih, T-H., Liou, W.W., Shabbir, A., Yang, Z. and Zhu, J., “A new  $\kappa - \epsilon$  eddy viscosity model for high Reynolds number turbulent flows”, *Computer & Fluids*, **24**, 227-238, 1995.
- [19] ANSYS, *ANSYS Mechanical*, ver. 16.1, computer program, ANSYS Inc, Canonsburg, Pennsylvania, 2015.